Magnesium Technology 2011
Edited by: Wim H. Sillekens, Sean R. Agnew, Neale R. Neelameggham, and Suveen N. Mathaudhu
TMS (The Minerals, Metals & Materials Society), 2011

Microstructures and Casting Defects of Magnesium Alloy Made By A New Type of Semisolid Injection Process

Yuichiro Murakami[1], Naoki Omura[1], Mingjun Li[1], Takuya Tamura[1], Shuji Tada[1], Kenji Miwa[1]
[1]Material Research Institute for Sustainable Development, National Institute of Advanced Industrial Science and Technology (AIST)
2266-98 Anagahora, Shimo-Shidami, Moriyama-ku, Nagoya 463-8560, Japan

Keywords: magnesium, semisolid, injection speed, fraction solid, microstructure, casting defect

Abstract

We have developed a new type of semisolid injection process that allows magnesium alloys to be formed in high material yields approximating 90%. In this process, generic magnesium billets are heated into their semisolid temperature range in an injection cylinder, without cover gas, and then the material is injected into a mold.

In this study, several billets were precision-heated in the cylinder to obtain a desired fraction solid. Plate specimens were produced by injecting the material at different injection speeds. Microstructures were observed by optical microscopy, and casting defects were detected on an X-ray computed tomography scanner. As injection speed was increased, the size and shape of α-Mg solid particles became smaller and more spherical, and the defect volume fraction increased. In contrast, as the fraction solid was increased, the defect volume fraction decreased. Spheroidization and miniaturization of solid particles were attributed to shear stress at the nozzle, and defects were affected by viscosity.

Introduction

In recent years, the development of environmental protection programs and green technology has become increasingly important. In particular, reducing carbon dioxide emissions and fuel efficiency improvement are urgent issues for the automobile industry, and vehicle weight reduction is one highly effective means of improving fuel efficiency. Hence, extensive research has been conducted on reducing vehicle weight. Toward this end, one approach is the expanded use of light metals such as aluminum and magnesium. Magnesium in particular is considered to be a promising lightweight structural material because it has the lowest density among applicable metallic materials, and has excellent specific strength. In recent years, magnesium alloy consumption has increased markedly, and it is expected that this growth trend will continue.

The die-casting process is among the most commonly used methods for forming magnesium alloys. However, components molded by die-casting exhibit low engineering performance due to the existence of inherent defect such as porosity, hot cracks and oxide inclusions. Additionally, die-casting of magnesium alloys requires the use of cover gas (e.g., SF_6) because magnesium alloys are easy combustible in the liquid state; However, SF_6 gas has a high global warming potential of about 24000, and thus its use should be avoided.

Recently, semisolid processes have been developed to fabricate high-quality aluminum alloy products [1 - 3]. The semisolid injection process uses a semisolid billet that has a higher viscosity than liquid metal; consequently, casting defects in the final components can be reduced. This process is useful for magnesium alloys because processing temperatures lower than conventional casting processes result in decreased combustibility of the magnesium alloy.

We have developed a new type of semisolid injection process that allows magnesium alloys form in high material yield of about 90% [4, 5]. In this process, generic magnesium billets are heated to the semisolid temperature range in an injection cylinder. Thus, the semisolid magnesium alloy is not exposed to air. For this reason, this process requires no cover gas usage.

In this study, an apparatus was developed for preparing specimens using the semisolid injection process. Plate specimens were prepared by injecting AZ91D semisolid billet into a permanent mold through a narrow nozzle. The effects of the volume fraction solid and injection speed on microstructures and casting defects were investigated.

Experimental procedure

A diagram of the semisolid forming apparatus is shown in Fig. 1. This experimental setup has a vertical injection system. The injection cylinder is able to heat the magnesium alloy billets to the semisolid temperature, as well as to maintain this temperature. The semisolid billet can then be injected into a permanent mold by a piston. The injection cylinder has an inner diameter of 25 mm, an outer diameter of 60 mm and a length of 54 mm; the

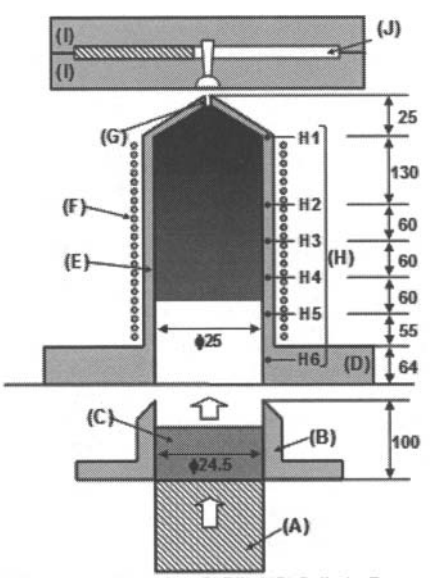

Fig. 1 Schematic representation of semisolid forming apparatus

nozzle is 3 mm in diameter. In this setup, the extrusion ratio is about 70. The injection cylinder is always filled with billets from the nozzle to a 320 mm height in the apparatus, and the billet in the uppermost part of the cylinder is heated to the semisolid temperature range.

The injection cylinder is equipped with six heaters on the surface of the outer wall; these heaters can control the temperature of the billet precisely. The six heaters are controlled independently on the basis of measurements from six thermocouples (H1 to H6), each of which is inserted at the location of a heater. The thermocouples measure the temperature of the cylinder wall, but this value is different from the actual temperature of the billet inside the cylinder. Therefore, the actual temperature of the billet was measured by inserting a thermocouple into the billet directly from the nozzle, in order to calibrate the heaters and thermocouples. Then, the temperature of the billet could be controlled precisely to obtain the optimal temperature balance from heaters H1 to H6. The temperature of the billet in the uppermost part of the injection cylinder (from the nozzle to 130 mm height) was set to a temperature in the semisolid range, namely, 591°C, 586°C or 581°C. The fraction solid f_s was 0.3, 0.4 or 0.5, respectively, at each of these temperatures. Meanwhile, the temperature of the billet was set lower, nearer to the bottom of the injection cylinder. The bottom of the billet was below the solidus temperature. Thus, the semisolid billet was not exposed to air; therefore, cover gas was not used in this experiment.

The billet was inserted into the magazine and moved directly under the cylinder by an air piston. The billet was then inserted into the injection cylinder by a hydraulic piston. The injection cylinder was continuously filled with billets, thus forcing semisolid billet from the uppermost part of the heated cylinder through the nozzle into the permanent mold. The injection speed was set to 220, 300 or 400 mm/s. The permanent mold had two plate cavities of 20 mm in width, 100 mm in length and 5 mm in thickness. In this experiment, one plate specimen was made per injection because one cavity was filled by dummy.

The specimens were polished by grinding with SiC paper, followed by polishing with diamond paste. Then, the specimens were etched in a solution of 75 ml ethylene glycol, 1 ml nitric acid and 24 ml distilled water. The microstructures of these specimens were observed by optical microscopy. Also, the specimens were analyzed on an X-ray computerized tomography (CT) scanner. The casting defects were detected from 3D volume images of specimens made from these X-ray images.

Results and discussion

Effects of fraction solid and injection speed on microstructure

Fig. 2 shows typical microstructures of AZ91D magnesium alloys injected under various conditions. These micrographs show that the AZ91D magnesium alloys had a homogeneous microstructure with a uniform dispersion of primary α-Mg in the matrix (eutectic α-Mg and β-$Mg_{17}Al_{12}$). We feel that the α-Mg particles were the solid phase and the matrix was the liquid phase when the slurry was injected. With increasing fraction solid, the size of primary solid particles increased and the primary solid particle shape changed from irregular to spherical.

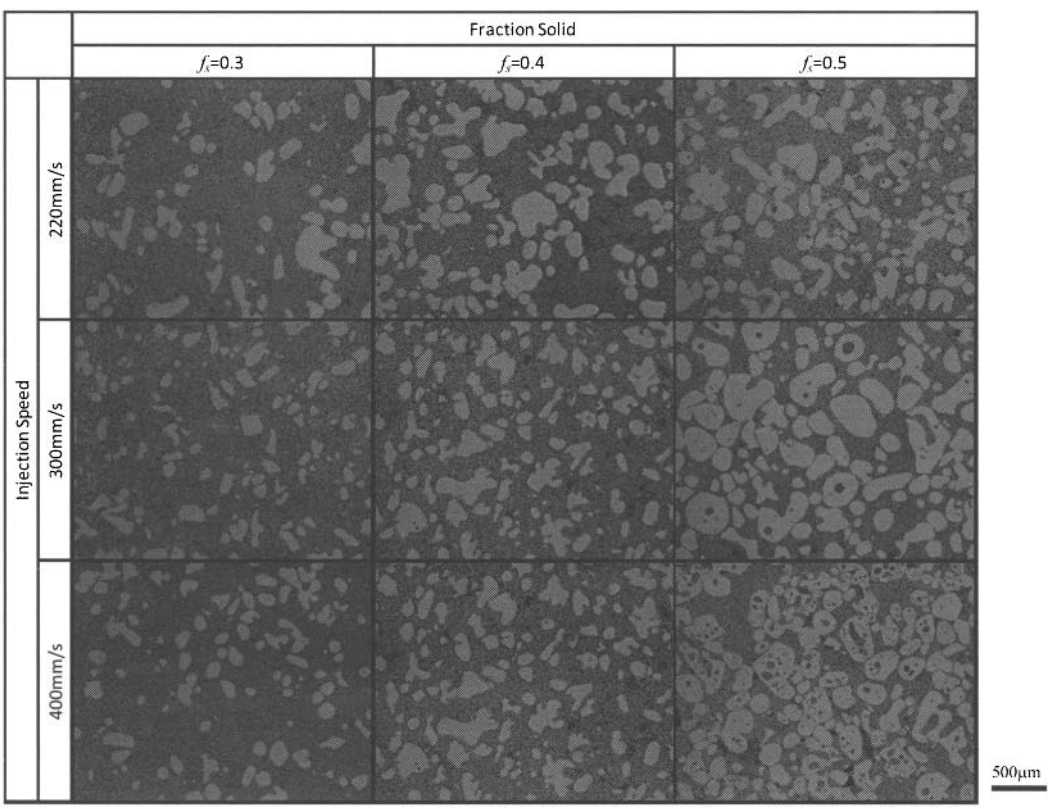

Fig. 2 Microstructure of AZ91D injected into a permanent mold

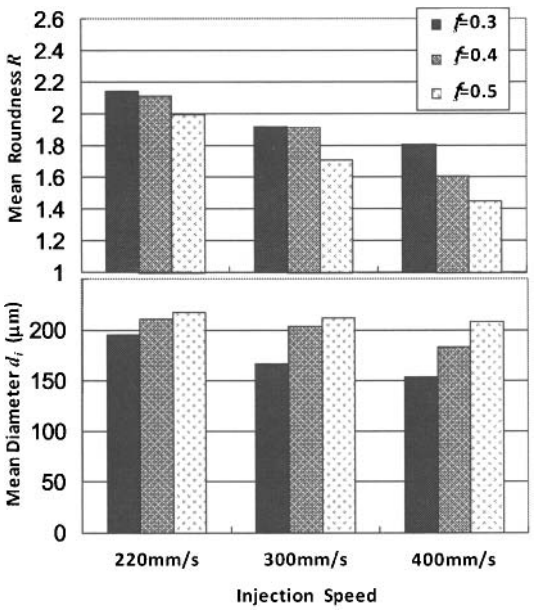

Fig. 3 Effect of injection speed and fraction solid on the mean roundness and diameter of primary α-Mg particle

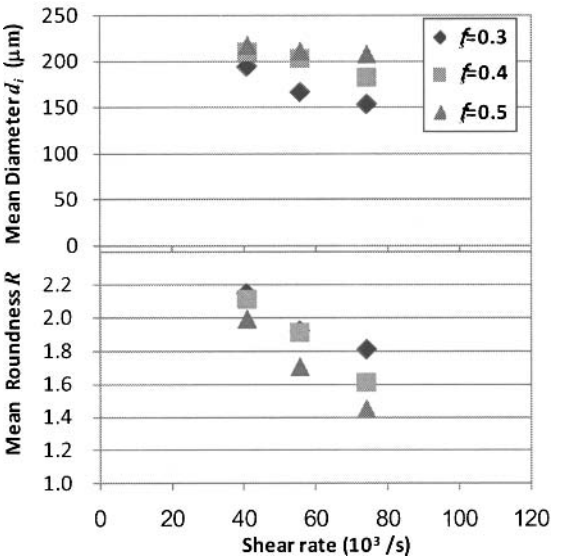

Fig. 4 Relations of mean diameter and roundness of primary α-Mg particles versus shear rate at the nozzle

The α-Mg particle diameter d [μm] (equivalent circle diameter) and the roundness R was measured at five locations of a specimen by image analysis.

Roundness was calculated as follows:

$$R = L^2/(4\pi A),$$

where L [μm] and A [μm^2] are the boundary length and area of an α-Mg particle. When R = 1, the particle is a true circle. Also, the area-weighted mean diameter d_s [μm] and area-weighted mean roundness R_s were calculated using the following equations:

$$d_s = \Sigma d_i A_i / \Sigma A_i$$

and

$$R_s = \Sigma R_i A_i / \Sigma A_i,$$

where d_i [μm], A_i [μm^2] and R_i are the diameter, area and roundness, respectively, of an α-Mg particle. Fig. 3 shows the weighted mean diameter d_s [μm] and area-weighted mean roundness R_s calculated as described above. These results show that increasing fraction solid or increasing injection speed decreased the mean roundness and increased the mean diameter of the α-Mg particles.

The shear rate and viscosity of slurry strongly affect the shear stress at the nozzle. Increasing the shear rate or viscosity increases shear stress. The shear rate γ [1/s] can be calculated from the injection speed S [m/s] and the dimensions of the nozzle and cylinder [6]:

$$\gamma = \frac{4Q}{\pi r_1^3}, \qquad (1)$$

where Q [m^3/s] is the flow rate through the nozzle given by $Q = \pi r_2^2 S$, r_1 [m] is the diameter of the nozzle, and r_2 [m] is the diameter of the cylinder.

Fig. 4 shows the relationships between mean particle roundness and shear rate, and between mean particle diameter and shear rate. The roundness and particle diameter decreased with increasing shear rate. In addition, for the same shear rate at the nozzle, particles became more spherical as the fraction solid increased. This result suggests that the primary solids were sheared through the nozzle during injection, and as a result became smaller and more spherical at high injection speeds. On the other hand, a high fraction solid increases shear stress, but particle size is affected by both shear stress and fraction solid. For this reason, particles became spherical with increasing fraction solid only at the same shear rate.

Effects of fraction solid and injection speed on casting defects

Fig. 5 shows the distribution of casting defects in the specimen prepared at an injection speed of 400 mm/s, as observed from X-ray CT images. In the case of zero fraction solid $f_s = 0$, many casting defects were dispersed throughout the specimen. It is considered that air in the mold was trapped in the specimen because this process is different from the die-casting process in that the mold has no overflows and runner. On the other hand, when semisolid material was injected, casting defects were significantly decreased. For fraction solid $f_s = 0.3$ and 0.4, the casting defects tended to be generated only in the middle of the specimen in the thickness direction. Additionally, many casting defects were dispersed throughout the specimens in the length direction and some of these had a crescent shape. In the semisolid injection process, it is known that the liquid-rich phase with higher fluidity is injected from nozzle to the end of the cavity first. After that, the solid-rich phase is injected into the cavity [7].

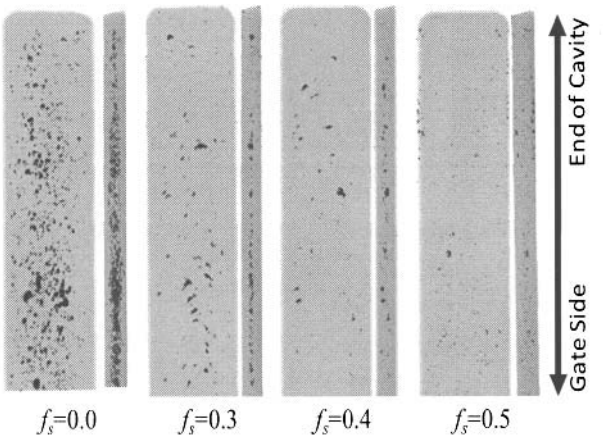

Fig. 5 Distribution of casting defects in the specimen prepared at the injection speed of 400 mm/s

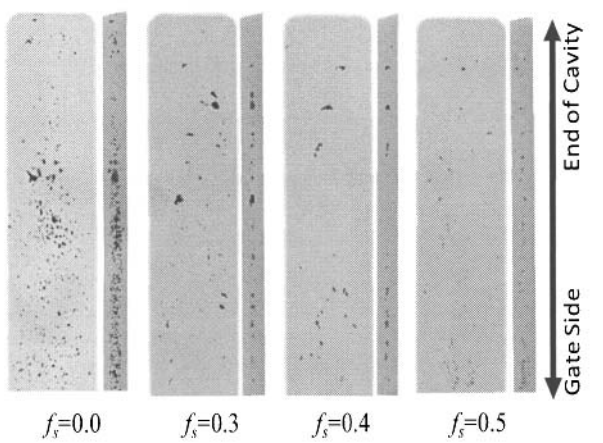

Fig. 6 Distribution of casting defects in the specimen prepared at the injection speed of 300 mm/s

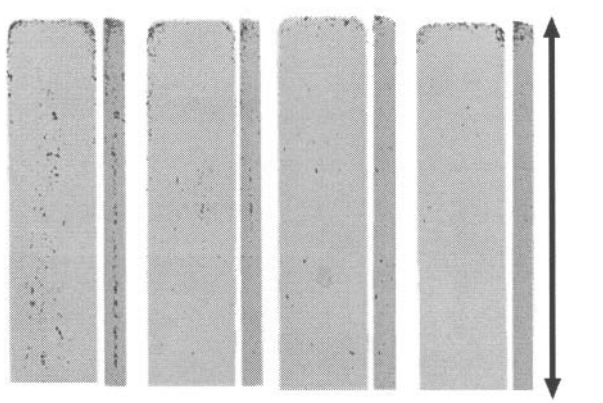

Fig. 7 Distribution of casting defects in the specimen prepared at the injection speed of 220 mm/s

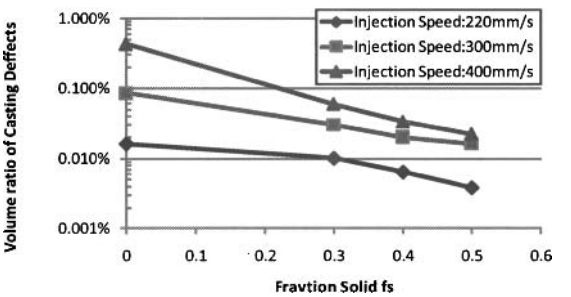

Fig. 8 Effects of fraction solid and injection speed on volume content of casting defects

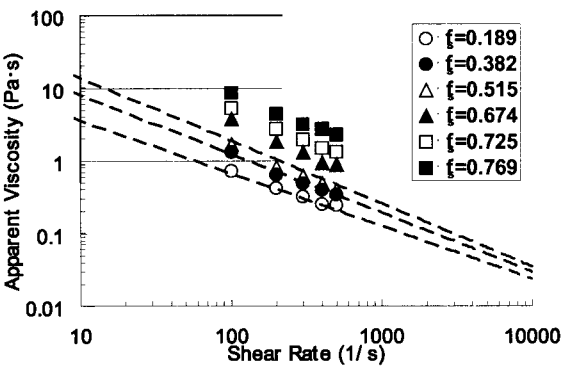

Fig. 9 Comparison of steady-state apparent viscosity with shear rate at various fraction solids for AZ91 [Error! Bookmark not defined.]. Dashed lines show approximate values calculated using Eq. (2).

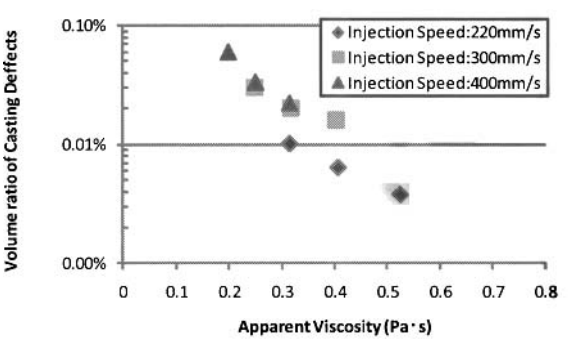

Fig. 10 Relationship between steady-state apparent viscosity in cavity and volume of casting defects

When the fraction solid is low, it is thought that the liquid-rich phase filled the air vents. For this reason, air in the mold was trapped in the specimen at the gap between the liquid-rich phase injected first and the solid-rich phase injected second.

Fig. 6 and Fig. 7 show the distribution of casting defects in the specimens prepared at injection speeds of 300 and 220 mm/s, respectively. At the injection speed of 300 mm/s, there were fewer casting defects in comparison with the injection speed of 400 mm/s for a given fraction solid. In addition, the shape of the defects exhibited the same tendency as in the case of an injection

speed if 400 mm/s. It appears that air was trapped in specimens prepared at 300 and 400 mm/s for the same reason. On the other hand, for the specimen prepared at an injection speed of 220 mm/s, casting defects in the center part of the specimen were significantly diminished. However, the number of small casting defects at the end of the cavity increased. It appears that the slurry fluidity was insufficient to fill the entire cavity when the injection speed was 220 mm/s.

Error! Reference source not found. Fig. 8 shows the defect volume content in the specimens in relation to their fraction solid. The volume ratio of the defects decreased with increasing fraction solid or decreasing injection speed. This seems to be attributable to the fact that the viscosity of the slurry increased as the fraction solid increased [8].

Ghosh et al. [9] have reported the effects of the shear rate and the fraction solid on the apparent viscosity of AZ91D at steady state. In their study, the apparent viscosity was measured with a coaxial-cylinder rheometer. At $f_s \leq 0.55$, the apparent viscosity η [Pa·s] of AZ91D in the steady state was approximated by the following equation:

$$\eta = 7.10\exp(5.17 f_s) \Big/ \dot{\gamma}^{(0.43 f_s + 0.64)}, \quad (2)$$

and the shear rate $\dot{\gamma}$ in the cavity can be calculated as

$$\dot{\gamma} = \frac{6Q}{L^2 D}, \quad (3)$$

where Q [m^3/s] is the flow rate through the nozzle given by $Q = \pi r^2 S$, r [m] is the diameter of the cylinder, and L [m] and D [m] are the width and thickness of the cavity, respectively.

Fig. 10 shows the relationship between the apparent viscosity in the cavity and the volume of casting defects. At injection speeds of 300 and 400 mm/s, the volume of casting defects similarly decreased with increasing the apparent viscosity. On the other hand, at the injection speed of 220 mm/s, the volume of casting defects significantly diminished in comparison to the injection speeds of 300 and 400 mm/s for the same viscosity. If the slurry does not reach a steady state, the apparent viscosity of slurry will be affected not only by the fraction solid and shear rate but also by particle morphology and particle agglomeration [10]. Fig. 3 showed that α-Mg particles in the slurry injected at 220 mm/s were not spherical. Thus, it appears that the viscosity of the slurry was less than that in the steady state. Hence, the volume of casting defects was significantly diminished. Additionally, for the injection speed of 220 mm/s, it was thought that the shear stress at the nozzle was insufficient for improving fluidity.

Conclusions

In order to investigate the effects of the fraction solid and injection speed on microstructure and casting defects, experiments on the semisolid forming of AZ91D magnesium were performed. The primary α-Mg particles became large and spherical with increasing fraction solid. Furthermore, with increasing injection speed, the size of the primary solid particle decreased and the shape of the primary solid particle became spherical. By calculating the shear rate at the nozzle, it was revealed that the roundness and diameter of α-Mg particles decreased with increasing shear stress. However, the fraction solid affected the diameter of α-Mg particles more strongly than shear stress.

The amount of casting defects decreased with increasing fraction solid or decreasing injection speed. For injection speeds of 300 and 400 mm/s, casting defects from trapped air were distributed throughout the specimen. On the other hand, for the injection speed of 220 mm/s, many casting defects were generated at the end of cavity because the fluidity of slurry was insufficient. For the injection speeds of 300 and 400 mm/s, the volume of casting defects was similarly decreased with increasing apparent viscosity. However, at the injection speed of 220 mm/s, the volume of casting defects was substantially reduced in comparison to the injection speeds of 300 and 400 mm/s for a given viscosity. The reason that the α-Mg particles in the slurry injected at 220 mm/s were not spherical is that shear stress at the nozzle was insufficient.

References

1. W.G. Cho and C.G. Kang, "Mechanical properties and their microstructure evaluation in the thixoforming process of semi-solid aluminum alloys," *Journal of Materials Processing Technology*, 105 (2000), 269-277

2. S. Nafisi and R. Ghomashchi, "Grain refining of conventional and semi-solid A356 Al–Si alloy," *Journal of Materials Processing Technology*, 174 (2006), 371-383

3. H.K. Jung and C.G. Kang, "Induction heating process of an Al–Si aluminum alloy for semi-solid die casting and its resulting microstructure," *Journal of Materials Processing Technology*, 174 (2006), 355-364

4. K. Miwa, R. Rachmat, T. Tamura and Y. Sakaguchi, "Relationship between volume fraction solid and casting defect on semi solid injection in AZ91D magnesium alloy," *Journal of Japan Foundry Engineering Society*, 78 (2006), 187-193 (in Japanese)

5. N. Omura, Y. Murakami, M.G. LI, T. Tamura and K. Miwa, "Effect of Volume Fraction Solid and Injection Speed on Mechanical Properties in New Type Semi-solid Injection Process," *Solid State Phenomena*, 141-143 (2008) 761-766

6. The Society of Polymer Science Japan, ed., *Plastic Processing Handbook* (Nikkan Kogyo Shimbun Ltd., 1995) 1401 (in Japanese)

7. R. Rachmat, T. Tamura and K. Miwa, "Fluidity and Microstructures Characteristics of AZ91D by using New Type Semi-solid Injection Process," *Solid State Phenomena*, 116-117 (2006) 534-537

8. D. B. Spencer, R. Mehrabian and M. C. Flemings, "Rheological behavior of Sn-15 Pct Pb in the Crystallization Range," Metallurgical Transactions, 3 (1972) 1925-1932

9. D. Ghosh, R. Fan and C. VanSchilt, "Thixotropic roperties of Semi-Solid Magnesium Alloys AZ91D and AM50," *Proceedings of The 3rd International Conference on Semi-Solid Processing of Alloys and Composites*, (1994) 85-94

10. M. C. Flemings, "Behavior of metal alloys in the semisolid state," *Metallurgical Transactions B*, 22B (1991) 269-293